

A finite thin circular beam element for out-of-plane vibration analysis of curved beams[†]

Bo Yeon Kim, Chang-Boo Kim*, Seung Gwan Song, Hyeon Gyu Beom and Chongdu Cho

Department of Mechanical Engineering, Inha University, 253 Yonghyun-dong, Nam-gu, Incheon, 402-751, Korea

(Manuscript Received December 20, 2007; Revised April 29, 2008; Accepted December 16, 2008)

Abstract

A finite thin circular beam element for the out-of-plane vibration analysis of curved beams is presented in this paper. Its stiffness matrix and mass matrix are derived, respectively, from the strain energy and the kinetic energy by using the natural shape functions derived from an integration of the differential equations in static equilibrium. The matrices are formulated with respect to the local polar coordinate system or to the global Cartesian coordinate system in consideration of the effects of shear deformation and rotary inertias. Some numerical examples are analyzed to confirm the validity of the element. It is shown that this kind of finite element can describe quite efficiently and accurately the out-of-plane motion of thin curved beams.

Keywords: Finite element; Mass matrix; Natural shape function; Out-of-plane vibration; Rotary inertia; Shear deformation; Stiffness matrix; Thin circular beam

1. Introduction

The out-of-plane vibration analysis of curved beams is quite complex due to the coupling effects of bending and torsion, transverse shear and rotary inertia force. Neglecting these effects may lead to inaccuracies in analysis, especially when the ratio of radial thickness to curvature radius of a curved beam is large (thick circular beam), or when the natural frequency is high for vibration problem even if the ratio of radial thickness to curvature radius is very small (thin circular beam).

Davis et al. [1] presented the shape functions of a curved beam element, which the effects of transverse shear deformation and transverse rotary inertia were considered. Their out-of-plane displacements were obtained from an integration of the differential equations of an infinitesimal element in static equilibrium. The stiffness and mass matrices were derived from

the force-displacement relations and the kinetic energy equations, respectively. The matrices are formulated in the local straight-beam (Cartesian) coordinate system rather than in the local curvilinear (polar) coordinate system, and thus a transformation of the matrices for the local coordinate system to the one for the common global coordinate system is required before they are assembled even though the radius of curvature for the entire curved beam is constant. Yoo and Fehrenbach [2] derived the stiffness and mass matrices of a spatial curved beam element by using the minimum potential energy theory, where the effects of warping and rotary inertia due to flexure and torsion were considered but the effects of shear deformation were neglected. Palaninathan and Chandrasekharan [3] derived the stiffness matrix for a spatial curved Timoshenko beam element by using Castigliano's theorem, where only the effects of shear deformation are considered. Lebeck and Knowlton [4] developed the stiffness matrix of a circular beam element using ring theory, where the in-plane motion is coupled with the out-of-plane motion due to the unsymmetrical cross-sectional area, but the effects of

[†] This paper was recommended for publication in revised form by Associate Editor Seockhyun Kim

* Corresponding author. Tel.: +82 32 860 7383, Fax.: +82 32 868 1716

E-mail address: kimcb@inha.ac.kr

© KSME & Springer 2009

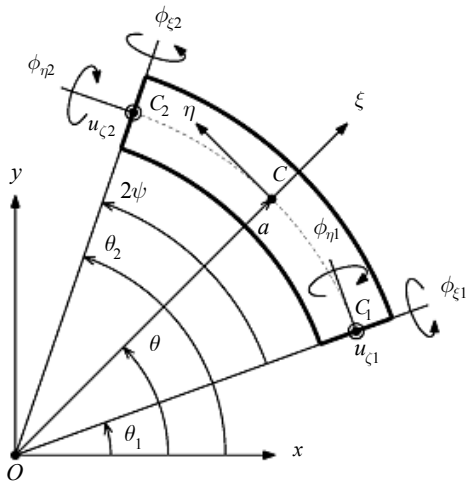


Fig. 1. The coordinate system of a circular beam element.

shear deformation are neglected.

Choi and Lim [5] also developed two general curved beam elements based on Timoshenko beam theory. The two-node element was formulated from constant strain fields and the three-node one was formulated from linear strain fields. The stiffness matrices were derived from the total potential energy theorem in the local curvilinear coordinate system and were transformed into the common global Cartesian coordinate system.

Wu and Chiang [6] derived the stiffness and mass matrices from the force-displacement relations and the kinetic energy equations, respectively. The shape functions were modified in order to consider the effect of shear deformation from the ones given by Lebeck and Knowlton [4]. The matrices are formed from the out-of-plane motions of a moderately thick curved beam with the effects of transverse shear deformation, transverse rotary inertia, and torsional rotary inertia.

In this paper, a finite thin circular beam element, which considers the effects of transverse shear deformation, transverse rotary inertia, and torsional rotary inertia, is presented. This kind of element can be used in the analysis of thin beam in which the effect of variation in curvature across the section can be neglected. Its stiffness and mass matrices are derived from the strain energy and the kinetic energy, respectively, in the same manner as the work of Kim et al. [7] for a thin circular beam element with in-plane motions. These matrices can be transformed easily into the global Cartesian coordinate system.

2. Thin circular beam element

2.1 Out-of-plane deformations

The global Cartesian coordinate system of a circular beam element is shown in Fig. 1. O is the center of curvature of the element. The cross section perpendicular to the circumferential direction of the element is doubly symmetric with respect to the $\xi-\eta$ plane and the $\eta-\zeta$ plane, and its area is uniform. The radius of the centroidal line passing through the center of cross section is a . Half of the subtended angle of the element is $\psi = (\theta_2 - \theta_1)/2$. The nodes of the element, C_1 and C_2 are on the centroidal line.

When only the out-of-plane deformations with respect to the $x-y$ plane of a circular beam are considered, the displacement of the center of cross section, C , at an angular position θ has axial component u_ζ with respect to a local polar coordinate system $C\xi\eta\zeta$. The rotation of the cross section at C has radial component ϕ_ξ and circumferential component ϕ_η which are supposed very small.

The bending curvature κ_ξ , twist τ_η , and shear strain γ_ζ at C of a circular beam are, respectively, as

$$\kappa_\xi = (\phi_{\xi,\theta} - \phi_\eta) / a \tag{1a}$$

$$\tau_\eta = (\phi_{\eta,\theta} + \phi_\xi) / a \tag{1b}$$

$$\gamma_\zeta = -\phi_\xi + u_{\zeta,\theta} / a \tag{1c}$$

where $(\)_{,\theta}$ is a partial differential with respect to circumferential coordinate θ .

For a thin beam, the radial thickness is very small as compared with the radius of centroidal line and the effect of variation in curvature across the cross section can be neglected. The internal bending moment M_ξ , torsional moment M_η , and shear force N_ζ at the point C can be expressed as

$$M_\xi = EI_\xi \kappa_\xi \tag{2a}$$

$$M_\eta = GJ_\eta \tau_\eta \tag{2b}$$

$$N_\zeta = K_\zeta GA \gamma_\zeta \tag{2c}$$

where A , I_ξ , J_η , and K_ζ are the area, the area moment of inertia about ξ -axis, the torsional moment of inertia (Sololnikoff [8]), and the shear coeffi-

cient of the cross section (Cowper [9]), respectively. E is Young's modulus of the material. G is the shear modulus, which is expressed as $G = E/2(1 + \nu)$ with the Poisson ratio ν .

2.2 Shape functions

Out-of-plane forces and moments are applied on the cross sections at nodes, C_1 and C_2 of the circular beam element in equilibrium.

The internal bending moment, torsional moment, and shear force on the cross section at C can be expressed with the internal bending moment M_{ξ_0} , torsional moment M_{η_0} , and shear force N_{ζ_0} on the mid cross section at $\phi = 0$ as

$$M_{\xi} = M_{\xi_0}c\phi + (M_{\eta_0} - aN_{\zeta_0})s\phi \tag{3a}$$

$$M_{\eta} = -M_{\xi_0}s\phi + (M_{\eta_0} - aN_{\zeta_0})c\phi + aN_{\zeta_0} \tag{3b}$$

$$N_{\zeta} = N_{\zeta_0} \tag{3c}$$

where

$$s\phi = \sin \phi, \quad c\phi = \cos \phi, \quad \phi = \theta - (\theta_2 + \theta_1)/2.$$

By substituting Eq. (3) into Eq. (2), the bending curvature, twist and shear strain at C can be expressed with the internal bending moment, the torsional moment, and the shear force on the mid cross section as

$$\kappa_{\xi} = (B_5c\phi + B_6s\phi)/a^2 \tag{4a}$$

$$\tau_{\eta} = \beta_{\eta}(B_4 - B_5s\phi + B_6c\phi)/a^2 \tag{4b}$$

$$\gamma_{\zeta} = \alpha_{\zeta}B_4/a \tag{4c}$$

where

$$B_4 = a^3N_{\zeta_0}/EI_{\xi} \tag{5a}$$

$$B_5 = a^2M_{\xi_0}/EI_{\xi} \tag{5b}$$

$$B_6 = a^2(M_{\eta_0} - aN_{\zeta_0})/EI_{\xi} \tag{5c}$$

$$\alpha_{\zeta} = EI_{\xi}/K_{\zeta}GAa^2 \tag{6a}$$

$$\beta_{\eta} = EI_{\xi}/GJ_{\eta} \tag{6b}$$

If $\alpha_{\zeta} = 0$, then the effect of transverse shear deformation is neglected, i.e., $\gamma_{\zeta} = 0$.

The radial rotation, circumferential rotation, and

axial displacement of the cross section at C , which are solutions of differential equations obtained by substituting Eq. (4) into Eq. (1), are expressed in terms of ϕ as

$$\phi_{\xi} = \{B_2c\phi + B_3s\phi + B_4f_2(1 - c\phi) + B_5(f_4s\phi + f_3\phi c\phi) + B_6f_3\phi s\phi\}/a \tag{7a}$$

$$\phi_{\eta} = \{-B_2s\phi + B_3c\phi + B_4f_2s\phi - B_5f_3\phi s\phi - B_6(f_4s\phi - f_3\phi c\phi)\}/a \tag{7b}$$

$$u_{\zeta} = B_1 + B_2s\phi - B_3c\phi + B_4(f_1\phi + f_2\phi - f_2s\phi) + B_5(-f_2 + f_2c\phi + f_3\phi s\phi) + B_6(f_2s\phi + f_4s\phi - f_3\phi c\phi) \tag{7c}$$

where

$$f_1 = \alpha_{\zeta} \tag{8a}$$

$$f_2 = \beta_{\eta} \tag{8b}$$

$$f_3 = (1 + \beta_{\eta})/2 \tag{8c}$$

$$f_4 = (1 - \beta_{\eta})/2 \tag{8d}$$

B_1 , B_2/a , and B_3/a are the constants of integration of the differential equations. They are the rigid body displacement of the center of curvature in the axial direction, the rigid body rotation about the center of curvature in the radial direction, and the rigid body rotation about the center of curvature in the circumferential direction at the mid cross section, respectively.

The static deformations represented by Eq. (7) are used as the shape functions for the out-of-plane motion of thin circular beam element. They are composed of the rigid body modes associated with B_1 , B_2/a , and B_3/a and the flexible modes associated with B_4 , B_5 , and B_6 . The flexible modes are null at $\phi = 0$.

The displacements and rotations at nodes, C_1 and C_2 , can be expressed as

$$\{v\} = [a]\{B\} \tag{9}$$

where

$$\{v\} = (\phi_{\xi_1} \quad \phi_{\eta_1} \quad u_{\zeta_1} \quad \phi_{\xi_2} \quad \phi_{\eta_2} \quad u_{\zeta_2})^T \tag{10a}$$

$$\{B\} = (B_1 \ B_2 \ B_3 \ B_4 \ B_5 \ B_6)^T \tag{10b}$$

$$[a] = \begin{bmatrix} 0 & c\psi/a & -s\psi/a & f_2(1-c\psi)/a \\ 0 & s\psi/a & c\psi/a & -f_2s\psi/a \\ 1 & -s\psi & -c\psi & -(f_1+f_2)\psi + f_2s\psi \\ 0 & c\psi/a & s\psi/a & f_2(1-c\psi)/a \\ 0 & -s\psi/a & c\psi/a & f_2s\psi/a \\ 1 & s\psi & -c\psi & (f_1+f_2)\psi - f_2s\psi \\ -(f_4s\psi + f_3\psi c\psi)/a & f_3\psi s\psi/a & & \\ -f_3\psi s\psi/a & (f_4s\psi + f_3\psi c\psi)/a & & \\ -f_2(1-c\psi) + f_3\psi s\psi & -(f_2+f_4)s\psi - f_3\psi c\psi & & \\ (f_4s\psi + f_3\psi c\psi)/a & f_3\psi s\psi/a & & \\ -f_3\psi s\psi/a & -(f_4s\psi - f_3\psi c\psi)/a & & \\ -f_2(1-c\psi) + f_3\psi s\psi & (f_2+f_4)s\psi - f_3\psi c\psi & & \end{bmatrix} \tag{10c}$$

The coefficient vector of shape functions, $\{B\}$ then can be expressed in terms of the nodal displacement vector with respect to the local polar coordinate system, $\{v\}$, as

$$\{B\} = [a]^{-1} \{v\} \tag{11}$$

The relationship between the nodal displacement vector with respect to the local polar coordinate system, $\{v\}$ and the nodal displacement vector with respect to the global Cartesian coordinate system, $\{\bar{v}\}$, is given by

$$\{v\} = [T] \{\bar{v}\} \tag{12}$$

where

$$\{\bar{v}\} = (\phi_{x1} \ \phi_{y1} \ u_{z1} \ \phi_{x2} \ \phi_{y2} \ u_{z2})^T \tag{13a}$$

$$[T] = \begin{bmatrix} c\theta_1 & s\theta_1 & 0 & 0 & 0 & 0 \\ -s\theta_1 & c\theta_1 & 0 & 0 & 0 & 0 \\ 0 & 0 & 1 & 0 & 0 & 0 \\ 0 & 0 & 0 & c\theta_2 & s\theta_2 & 0 \\ 0 & 0 & 0 & -s\theta_2 & c\theta_2 & 0 \\ 0 & 0 & 0 & 0 & 0 & 1 \end{bmatrix} \tag{13b}$$

2.3 Stiffness matrix

The strain energy of the thin circular beam element is

$$V = \frac{1}{2} \int_{\theta_1}^{\theta_2} (EI_{\xi} \kappa_{\xi}^2 + GJ_{\eta} \tau_{\eta}^2 + K_{\zeta} GA \gamma_{\zeta}^2) a d\theta \tag{14}$$

By substituting Eq. (4) into Eq. (14), the strain energy can be expressed in terms of the coefficient vector of shape functions as

$$V = \frac{1}{2} \{B\}^T [K_B] \{B\} \tag{15}$$

where $[K_B]$ is the stiffness matrix with respect to $\{B\}$ of the thin circular beam element. The elements of the symmetric matrix $[K_B]$ are detailed in the Appendix.

By substituting Eq. (11) into Eq. (15), the strain energy is expressed in terms of the nodal displacement vector in the local polar coordinate system as

$$V = \frac{1}{2} \{v\}^T [K] \{v\} \tag{16}$$

where $[K]$ is the stiffness matrix with respect to $\{v\}$ of the thin circular beam element as

$$[K] = [a]^{-T} [K_B] [a]^{-1} \tag{17}$$

If necessary, the stiffness matrix in the local polar coordinate system can be transformed into the global Cartesian coordinate system as follows:

$$[\bar{K}] = [T]^T [K] [T] \tag{18}$$

2.4 Mass matrix

The kinetic energy of the thin circular beam element is expressed as

$$T = \frac{1}{2} \int_{\theta_1}^{\theta_2} (\rho I_{\xi} \dot{\phi}_{\xi}^2 + \rho I_{\eta} \dot{\phi}_{\eta}^2 + \rho A \dot{u}_{\zeta}^2) a d\theta \tag{19}$$

where ρ is the density of the material. I_{η} is the area moment of inertia about η -axis of the cross section. (\cdot) is the partial differential with respect to time t .

By substituting Eq. (7) into Eq. (19), the kinetic energy is expressed in terms of the coefficient vector of

shape functions as

$$T = \frac{1}{2} \{\dot{B}\}^T [M_B] \{\dot{B}\} \quad (20)$$

where $[M_B]$ is the mass matrix with respect to $\{B\}$ of the thin circular beam element. The elements of the symmetric matrix $[M_B]$ are detailed in Appendix.

$$\mu_\xi = \rho I_\xi / \rho A a^2 \quad (21a)$$

$$\mu_\eta = \rho I_\eta / \rho A a^2 \quad (21b)$$

If the effect of transverse rotary inertia is neglected, then $\mu_\xi = 0$, i.e. $\rho I_\xi = 0$. If the effect of torsional rotary inertia is neglected, then $\mu_\eta = 0$, i.e., $\rho I_\eta = 0$.

By substituting Eq. (11) into Eq. (20), the kinetic energy is expressed in terms of the nodal displacement vector in the local polar coordinate system as

$$T = \frac{1}{2} \{\dot{v}\}^T [M] \{\dot{v}\} \quad (22)$$

where $[M]$ is the mass matrix with respect to $\{v\}$ of the element as

$$[M] = [a]^{-T} [M_B] [a]^{-1} \quad (23)$$

If necessary, the mass matrix in the local polar coordinate system can be transformed into the global Cartesian coordinate system as follows:

$$[\bar{M}] = [T]^T [M] [T] \quad (24)$$

2.5 Out-of-plane internal forces

By substituting Eq. (4) into Eq. (2) or from Eqs. (3) and (5), the internal bending moment, torsional moment, and shear force on the cross section at C can be expressed by the coefficients of shape functions as

$$M_\xi = (EI_\xi / a^2) (B_5 c\phi + B_6 s\phi) \quad (25a)$$

$$M_\eta = (EI_\xi / a^2) (B_4 - B_5 s\phi + B_6 c\phi) \quad (25b)$$

$$N_\zeta = (EI_\zeta / a^3) B_4 \quad (25c)$$

3. Validity of the beam element

3.1 Linear static analysis for a quarter cantilever ring with tip load

A quarter cantilever ring subjected to an axial tip load P is shown in Fig. 2. Its displacements can be obtained analytically from Eqs. (3), (5) and (7) by considering the geometric and natural boundary conditions at the two ends. The radial rotation $\phi_{\xi T}$, circumferential rotation $\phi_{\eta T}$, and axial displacement $u_{\zeta T}$ at the tip are

$$\phi_{\xi T} = \left(\frac{a^2}{EI_\xi} \right) \left\{ \frac{1}{2} (1 + \beta_\eta) \right\} P \quad (26a)$$

$$\phi_{\eta T} = \left(\frac{a^2}{EI_\xi} \right) \left\{ \beta_\eta - \frac{\pi}{4} (1 + \beta_\eta) \right\} P \quad (26b)$$

$$u_{\zeta T} = \left(\frac{a^3}{EI_\zeta} \right) \left\{ [\alpha_\zeta + \frac{1}{2} (1 + 3\beta_\eta)] \frac{\pi}{2} - 2\beta_\eta \right\} P \quad (26c)$$

The results of analytical solutions for the tip rotation and displacement, for which the effects of transverse shear deformation are considered and those effects are neglected, are summarized in Table 1. The same results as in Table 1 can be obtained by using FEM to model the quarter rings with only one, two or 16 thin circular beam elements because the shape functions of the element presented in this paper are exact in static state. In our calculations, the following factor and parameters are adopted: $E = 200$ GPa, $\nu = 0.25$, $\rho = 7830$ kg/m³, $a = 1$ m, $A = 6 \times 10^{-3}$ m², $I_\xi = 1.8 \times 10^{-6}$ m⁴, $I_\eta = 6.8 \times 10^{-6}$ m⁴, $J_\eta = 4.506 \times 10^{-6}$ m⁴, $K_\zeta = 0.847$

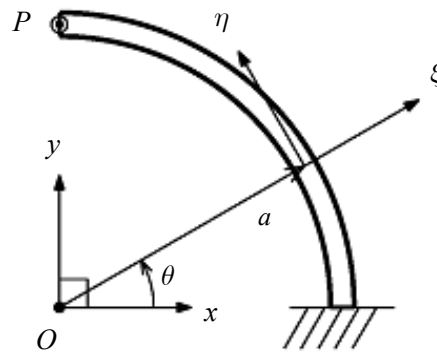


Fig. 2. A quarter cantilever ring subjected an axial tip load.

3.2 Natural vibration analysis for a free ring

The out-of-plane displacements of a ring, which is freely vibrating in a mode having n nodal diameters with a frequency of ω , will take the forms

$$\phi_\zeta = (\Phi_{\zeta C} \cos n\theta + \Phi_{\zeta S} \sin n\theta)e^{i\omega t} \quad (27a)$$

$$\phi_\eta = (\Phi_{\eta C} \cos n\theta + \Phi_{\eta S} \sin n\theta)e^{i\omega t} \quad (27b)$$

$$u_\zeta = (U_{\zeta C} \cos n\theta + U_{\zeta S} \sin n\theta)e^{i\omega t} \quad (27c)$$

The natural vibration equations can be obtained by substituting Eq. (27) into Eq. (14) and Eq. (19), integrating around the ring and applying Lagrange’s equations. For $n \geq 1$, there exist two orthogonal modes of which the natural frequencies are same, and the nodal diameters of one mode are rotated by $\pi/2n$ from the nodal diameters of the other. The above theoretical results are similar to the ones obtained by the previous works (Rao [10]; Kirkhope [11]).

In order to show the convergence of the thin circular beam element presented in this paper, the natural frequencies of the out-of-plane vibration of a free ring

Table 1. Tip rotations and displacement per unit axial tip load of a quarter cantilever ring.

	$\alpha_\zeta \neq 0$	$\alpha_\zeta = 0$
$\phi_{\zeta T}/P$ (rad/N)	2.7759×10-6	2.7759×10-6
$\phi_{\eta T}/P$ (rad/N)	-1.5863×10-6	-1.5863×10-6
$u_{\zeta T}/P$ (m/N)	3.1736×10-6	3.1698×10-6

* $\alpha_\zeta = 0$: neglecting the effect of transverse shear deformation.

are computed by using FEM to model the complete ring with 16, 32, 48, or 64 elements, and consider all the effects of transverse shear deformation, transverse rotary inertia, and torsional rotary inertia. The lowest eight natural frequencies of the flexible modes computed by using FEM are presented and compared with the theoretical values in Table 2. The first mode for $n = 0$ is translational rigid body mode and the second mode for $n = 1$ is rotational rigid body mode. It is shown that the natural frequencies computed by using FEM converged rapidly to the theoretical values with increasing number of elements. The errors in the natural frequencies increase with the number of nodal diameters and the order of frequencies.

To determine the effects of transverse shear deformation, transverse rotary inertia, and torsional rotary inertia on the natural frequencies of the out-of-plane vibration, the natural frequencies of a free ring are computed by using FEM to model the complete ring with 80 elements and consider the effects of transverse shear deformation, transverse rotary inertia, and torsional rotary inertia. Some natural frequencies of the flexible modes computed by using FEM are presented and compared with the theoretical values in Tables 3 and 4. When the effect of torsional rotary inertia is neglected, the second natural frequencies of some models in Table 3 disappear because the modes corresponding to the second frequencies are torsion-dominant modes. It is shown that the natural frequencies computed by using FEM are very accurate as compared with the theoretical values in the all cases. It is also shown that the errors in the natural frequencies increase with the number of nodal diameters and

Table 2. Convergence of natural frequencies of the out-of-plane vibration of a ring.

Number of nodal diameter n	Theory (Hz)	FEM (Hz) / Error (%)			
		16 elements	32 elements	48 elements	64 elements
2	37.283	37.289 / 0.016	37.283 / 0.002	37.283 / 0.001	37.283 / 0.000
3	105.11	105.24 / 0.123	105.13 / 0.014	105.12 / 0.005	105.12 / 0.002
4	200.70	201.58 / 0.436	200.80 / 0.050	200.74 / 0.017	200.72 / 0.009
5	322.89	326.40 / 1.089	323.30 / 0.129	323.03 / 0.044	322.96 / 0.022
0	413.84	416.50 / 0.643	414.51 / 0.160	414.14 / 0.071	414.01 / 0.040
6	470.72	481.11 / 2.208	472.00 / 0.271	471.16 / 0.094	470.94 / 0.047
1	585.27	592.75 / 1.278	587.15 / 0.320	586.11 / 0.142	585.74 / 0.080
7	643.22	667.68 / 3.804	646.43 / 0.499	644.34 / 0.174	643.79 / 0.088

Table 3. Comparison of natural frequencies of the out-of-plane vibration of a ring considering the effect of torsional rotary inertia.

Number of nodal diameter n	$\alpha_c \neq 0, \mu_c \neq 0$		$\alpha_c \neq 0, \mu_c = 0$		$\alpha_c = 0, \mu_c \neq 0$	
	Theory (Hz)	FEM (Hz) / Error (%)	Theory (Hz)	FEM (Hz) / Error (%)	Theory (Hz)	FEM (Hz) / Error (%)
2	37.283	37.283 / 0.000	37.305	37.305 / 0.000	37.312	37.312 / 0.000
3	105.11	105.12 / 0.001	105.25	105.26 / 0.001	105.41	105.41 / 0.000
4	200.70	200.71 / 0.005	201.17	201.18 / 0.005	201.86	201.86 / 0.001
5	322.89	322.93 / 0.014	324.05	324.09 / 0.014	325.97	325.97 / 0.002
0	413.84	413.95 / 0.026	413.84	413.95 / 0.026	413.84	413.95 / 0.026
6	470.72	470.86 / 0.029	473.11	473.24 / 0.029	477.37	477.39 / 0.003
1	585.27	585.57 / 0.051	585.27	585.57 / 0.051	585.79	586.09 / 0.051
7	643.22	643.56 / 0.053	647.55	647.91 / 0.054	655.74	655.78 / 0.006
8	839.33	840.09 / 0.091	846.53	847.32 / 0.093	860.72	860.82 / 0.011
2	925.91	927.09 / 0.128	925.91	927.09 / 0.128	927.22	928.41 / 0.128
9	1057.9	1059.5 / 0.143	1069.1	1070.7 / 0.148	1092.0	1092.2 / 0.017
10	1297.9	1300.7 / 0.215	1314.3	1317.2 / 0.223	1349.1	1349.4 / 0.027
3	1309.8	1313.2 / 0.257	1309.8	1313.2 / 0.257	1311.9	1315.3 / 0.257
11	1558.0	1562.8 / 0.308	1581.0	1586.1 / 0.321	1631.6	1632.2 / 0.039
4	1708.0	1715.4 / 0.437	1708.0	1715.4 / 0.437	1710.8	1718.3 / 0.437
12	1837.0	1844.8 / 0.426	1868.1	1876.5 / 0.447	1939.0	1940.1 / 0.055

* $\alpha_c = 0$: neglecting the effect of transverse shear deformation.

* $\mu_c = 0$: neglecting the effect of transverse rotary inertia.

Table 4. Comparison of natural frequencies of the out-of-plane vibration of a ring neglecting the effect of torsional rotary inertia.

Number of nodal diameter n	$\alpha_c \neq 0, \mu_c \neq 0$		$\alpha_c \neq 0, \mu_c = 0$		$\alpha_c = 0, \mu_c \neq 0$	
	Theory (Hz)	FEM (Hz) / Error (%)	Theory (Hz)	FEM (Hz) / Error (%)	Theory (Hz)	FEM (Hz) / Error (%)
2	37.336	37.337 / 0.000	37.359	37.359 / 0.000	37.366	37.366 / 0.000
3	105.30	105.31 / 0.001	105.45	105.45 / 0.002	105.60	105.60 / 0.000
4	201.10	201.11 / 0.005	201.57	201.58 / 0.005	202.26	202.27 / 0.001
5	323.55	323.59 / 0.014	324.71	324.76 / 0.014	326.66	326.67 / 0.001
6	471.70	471.83 / 0.029	474.10	474.23 / 0.029	478.42	478.43 / 0.003
7	644.56	644.90 / 0.054	648.92	649.27 / 0.055	657.21	657.25 / 0.006
8	841.07	841.84 / 0.091	848.32	849.11 / 0.093	862.71	862.80 / 0.010
9	1060.1	1061.6 / 0.144	1071.4	1072.9 / 0.148	1094.5	1094.7 / 0.016
10	1300.5	1303.3 / 0.215	1317.0	1320.0 / 0.223	1352.3	1352.6 / 0.025
11	1561.1	1565.9 / 0.308	1584.3	1589.4 / 0.322	1635.6	1636.2 / 0.037
12	1840.7	1848.5 / 0.427	1872.0	1880.3 / 0.448	1943.9	1944.9 / 0.052

the order of frequencies and neglecting the effects of transverse shear deformation, transverse rotary inertia, and torsional rotary inertia can increase the values of

natural frequencies of the ring, especially for the higher number of nodal diameters.

Table 5. Comparison of frequency parameters of the out-of-plane vibration of a circular arc.

s_ξ	Mode number	$\Phi = 60^\circ$		$\Phi = 120^\circ$		$\Phi = 180^\circ$	
		Theory*	FEM/ Error (%)	Theory*	FEM/ Error (%)	Theory*	FEM/ Error (%)
20	1	16.885	16.885/ 0.002	4.3094	4.3094/ 0.001	1.7908	1.7908/ 0.003
	2	39.700	39.706/ 0.014	11.796	11.796/ 0.001	5.0324	5.0324/ 0.001
	3	40.934	40.940/ 0.015	22.510	22.511/ 0.006	10.232	10.232/ 0.003
	4	70.581	70.612/ 0.043	23.303	23.304/ 0.003	16.917	16.918/ 0.005
100	1	19.454	19.454/-0.001	4.4731	4.4731/ 0.000	1.8182	1.8182/-0.001
	2	54.148	54.148/ 0.001	12.892	12.892/-0.002	5.2415	5.2415/ 0.000
	3	105.86	105.87/ 0.005	26.081	26.081/-0.001	10.989	10.989/-0.001
	4	173.16	173.18/ 0.010	43.684	43.684/ 0.001	18.813	18.813/ 0.002

* taken from (Howson et al., 1999)

3.3 Natural vibration analysis for circular arcs

The natural frequencies of the out-of-plane vibration for clamped-clamped circular arcs with circular cross-section are computed by using FEM by considering all the effects of shear and rotary inertia. The circular arcs were modeled with the circular beam elements with subtended angle of 1° .

For the comparison of the numerical results by FEM with the theoretical ones, which are presented in the works of Howson et al. [12], the shear coefficient of circular cross-section K_ζ is 0.89, and Poisson ratio ν is 0.3.

Table 5 shows that the natural frequencies computed by using FEM are very accurate as compared with the theoretical ones for all the two slenderness ratios and the three arc angles. The slenderness ratios s_ξ and frequency parameters λ in the table 5 are defined as

$$s_\xi = \sqrt{Aa^2 / I_\xi} \tag{28}$$

$$\lambda = \omega \sqrt{\rho Aa^4 / EI_\xi} \tag{29}$$

3.4 Natural vibration analysis for an S shaped beam

The natural frequencies of the out-of-plane vibration for a clamped-clamped S shaped beam composed of two identical half-rings with circular cross-section are computed by using FEM by considering all the effects of shear and rotary inertia. The beam was modeled with 360 and 36 circular beam elements and straight beam elements. Its properties are the same as the ones of the above clamped-clamped circular arc

Table 6. Comparison of frequency parameters of the out-of-plane vibration of an S-shaped beam.

Mode number	Using circular beam elements		Using straight beam elements	
	360 elements	36 elements	360 elements	36 elements
1	0.59431	0.59431	0.59385	0.59741
2	0.88651	0.88651	0.88588	0.89084
3	2.3955	2.3956	2.3933	2.4171
4	3.4674	3.4678	3.4638	3.5160
5	6.1575	6.1597	6.1491	6.2894
6	8.2507	8.2561	8.2390	8.4759

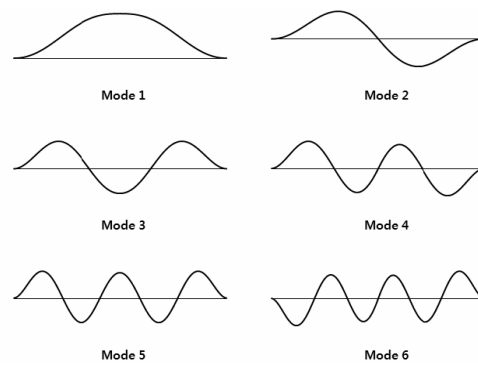


Fig. 3. Out-of-plane displacements of mode shapes along the S-shaped beam curve.

with $s_\xi = 20$.

Table 6 shows that the presented circular beam element for the natural vibration analysis gives good convergence and accuracy as compared with the

straight beam element.

The S-shaped beam has cyclic symmetry. As shown in Fig. 3, modes 1, 3, and 5 are axially symmetric modes with zero nodal diameter and modes 2, 4, and 6 are axially anti-symmetric modes with one nodal diameter.

4. Conclusions

A finite thin circular beam element for the out-of-plane vibration analysis of curved beams is presented. It can describe quite efficiently and accurately the out-of-plane motions of thin circular beams in which the secondary effects of transverse shear deformation, transverse rotary inertia, and torsional rotary inertia can be considered partially or totally. This kind of beam element gives exact results for linear static problems in the case of concentrated loads because the shape functions of the element are exact in static state. The natural frequencies obtained by using this kind of element converge rapidly to the theoretical values with increasing number of elements. The numerical results for the natural frequencies of circular arcs of various geometric conditions are in excellent agreement with the theoretical ones. The presented circular beam element can be utilized easily and efficiently for precise out-of-plane vibration analysis of curved beams composed of circular arcs.

Acknowledgment

This work was supported by Inha University Research Grant.

References

- [1] R. Davis, R. D. Henshell and G. B. Warburton, Curved beam finite elements for coupled bending and torsional vibration, *Earth. Eng. and Struct. Dynamics* 1 (1972) 165-175.
- [2] C. H. Yoo and J. P. Ferenbach, Natural frequencies of curved girders, *J. Eng. Mech. Div. ASCE* 107 (EM2) (1981) 339-354.
- [3] R. Palaninathan and P. S. Chandrasekharan, Curved beam element stiffness matrix formulation, *Comp. and Struct.* 21 (4) (1985) 663-669.
- [4] A. O. Lebeck and J. S. Knowlton, A finite element for the three-dimensional deformation of a circular ring, *Int. J. Num. Methods Eng.* 21 (1985) 421-435.
- [5] J. K. Choi and J. K. Lim, General curved beam elements based on the assumed strain fields, *Comp. and Struct.* 55 (3) (1995) 379-386.
- [6] J. S. Wu and L. K. Chiang, Out-of-plane responses of a circular curved Timoshenko beam due to a moving load, *Int. J. Solids Structures* 40 (2003) 7425-7448.
- [7] C. B. Kim, J. W. Park, S. Kim and C. Cho, A finite thin circular beam element for in-plane vibration analysis of curved beams, *J. Mech. Sci. and Tech.* 19 (12) (2005) 2187-2196.
- [8] I. S. Sokolnikoff, *Mathematical Theory of Elasticity*, McGraw-Hill, New York, USA, (1956).
- [9] G. R. Cowper, The shear coefficient in Timoshenko's beam theory, *J. Appl. Mech.* 33 (1966) 335-340.
- [10] S. S. Rao, Effects of transverse shear and rotary inertia on the coupled twist-bending vibrations of circular rings, *J. Sound Vibration.* 16 (4) (1971) 551-566.
- [11] J. Kirkhope, Out-of-plane vibration of thick circular ring, *J. Eng. Mech. Div. ASCE* 102 (EM2) (1976) 239-247.
- [12] W. P. Howson and A. K. Jemah, Exact out-of-plane natural frequencies of curved Timoshenko beams, *J. Eng. Mech.* 125 (1) (1999) 19-25.

Appendix

The matrix $[K_B]$ is symmetric and any element not defined is zero.

$$\begin{aligned}
 K_{Bij} &= (EI_\zeta / a^3) k_{Bij} \\
 k_{B44} &= 2(\beta_\eta + \alpha_\zeta) \psi \\
 k_{B46} &= 2\beta_\eta s \psi \\
 k_{B55} &= (\psi + s\psi c \psi) + \beta_\eta (\psi - s\psi c \psi) \\
 k_{B66} &= (\psi - s\psi c \psi) + \beta_\eta (\psi + s\psi c \psi)
 \end{aligned}$$

The matrix $[M_B]$ is symmetric and any element not defined is zero.

$$\begin{aligned}
 M_{Bij} &= (\rho A a) m_{Bij} \\
 m_{B11} &= 2\psi \\
 m_{B13} &= -2s\psi \\
 m_{B15} &= -2f_2(\psi - s\psi) + 2f_3(s\psi - \psi c \psi) \\
 m_{B22} &= 2\mu_\zeta \psi + (1 - \mu_\zeta + \mu_\eta)(\psi - s\psi c \psi)
 \end{aligned}$$

$$m_{B24} = -2\mu_\xi f_2(\psi - s\psi) + 2(f_1 + f_2)(s\psi - \psi c\psi) - (1 - \mu_\xi + \mu_\eta) f_2(\psi - s\psi c\psi)$$

$$m_{B26} = -\frac{1}{2}(1 - \mu_\xi + \mu_\eta) f_3(s\psi c\psi - \psi c2\psi) + (\mu_\eta f_4 + f_2 + f_4)(\psi - s\psi c\psi)$$

$$m_{B33} = 2\mu_\xi \psi + (1 - \mu_\xi + \mu_\eta)(\psi + s\psi c\psi)$$

$$m_{B35} = -\frac{1}{2}(1 - \mu_\xi + \mu_\eta) f_3(s\psi c\psi - \psi c2\psi) - 2f_2(\psi - s\psi) + (\mu_\xi f_4 + f_2)(\psi - s\psi c\psi)$$

$$m_{B44} = 4\mu_\xi f_2^2(\psi - s\psi) + (f_1 + f_2)^2 \frac{2}{3} \psi^3 - 4(f_1 + f_2) f_2(s\psi - \psi c\psi) + (1 - \mu_\xi + \mu_\eta) f_2^2(\psi - s\psi c\psi)$$

$$m_{B46} = 2\{\mu_\xi f_2 f_3 + (f_1 + f_2)(f_2 + f_4)\}(s\psi - \psi c\psi) - (\mu_\eta f_4 + f_2 + f_4) f_2(\psi - s\psi c\psi) + \frac{1}{2}(1 - \mu_\xi + \mu_\eta) f_2 f_3(s\psi c\psi - \psi c2\psi) - 2(f_1 + f_2) f_3(\psi^2 s\psi + 2\psi c\psi - 2s\psi)$$

$$m_{B55} = 4f_2^2(\psi - s\psi) + (\mu_\xi f_4^2 - f_2^2)(\psi - s\psi c\psi) - 4f_2 f_3(s\psi - \psi c\psi) + (\mu_\xi f_4 + f_2) f_3(s\psi c\psi - \psi c2\psi)$$

$$+ (1 - \mu_\xi + \mu_\eta) f_3^2 \left(\frac{1}{3} \psi^3 - \frac{1}{2} \psi^2 s2\psi - \frac{1}{2} \psi c2\psi + \frac{1}{4} s2\psi \right) + \mu_\xi f_3^2 \frac{2}{3} \psi^3$$

$$m_{B66} = \left\{ \mu_\eta f_4^2 + (f_2 + f_4)^2 \right\} (\psi - s\psi c\psi) - (\mu_\eta f_4 + f_2 + f_4) f_3(s\psi c\psi - \psi c2\psi) + (1 - \mu_\xi + \mu_\eta) f_3^2 \left(\frac{1}{3} \psi^3 + \frac{1}{2} \psi^2 s2\psi + \frac{1}{2} \psi c2\psi - \frac{1}{4} s2\psi \right) + \mu_\xi f_3^2 \frac{2}{3} \psi^3$$



Chang-Boo Kim received his B.S. degree in Mechanical Engineering from Seoul University, Korea in 1973. He then received his D.E.A., Dr.-Ing. and Dr.-es-Science degrees from Nantes University, France in 1979, 1981 and 1984, respectively.

Dr. Kim is currently a Professor at the School of Mechanical Engineering at Inha University in Incheon, Korea. His research interests are in the area of vibrations, structural dynamics, and MEMS.